Chinese Chemical Letters 34 (2023) 107451

Contents lists available at ScienceDirect

Chinese Chemical Letters

journal homepage: www.elsevier.com/locate/cclet

Novel 3D printed shape-memory PLLA-TMC/GA-TMC scaffolds for bone tissue engineering with the improved mechanical properties and degradability

Xulin Hu[a], Weiming Zhao[a], Zhen Zhang[a], Jianping Xie[a], Jian He[d], Jianfei Cao[e], Qing Li[b], Yajing Yan[a], Chengdong Xiong[b,c,*], Kainan Li[a,*]

[a] Clinical Medical College & Affiliated Hospital of Chengdu University, Chengdu University, Chengdu 610081, China
[b] Chengdu Institute of Organic Chemistry, Chinese Academy of Sciences, Chengdu 610041, China
[c] University of Chinese Academy of Sciences, Beijing 100049, China
[d] College of Medical, Henan University of Science and Technology, Luoyang 471023, China
[e] School of Materials and Environmental Engineering, Chengdu Technological University, Chengdu 610031, China

ARTICLE INFO

Article history:
Received 14 January 2022
Revised 5 April 2022
Accepted 19 April 2022
Available online 23 April 2022

Keywords:
Bone scaffolds
Biodegradable polymers
3D printed
Shape memory
Tissue engineering

ABSTRACT

The biodegradable substitution materials for bone tissue engineering have been a research hotspot. As is known to all, the biodegradability, biocompatibility, mechanical properties and plasticity of the substitution materials are the important indicators for the application of implantation materials. In this article, we reported a novel binary substitution material by blending the poly(lactic-acid)-*co*-(trimethylene-carbonate) and poly(glycolic-acid)-*co*-(trimethylene-carbonate), which are both biodegradable polymers with the same segment of flexible trimethylene-carbonate in order to accelerate the degradation rate of poly(lactic-acid)-*co*-(trimethylene carbonate) substrate and improve its mechanical properties. Besides, we further fabricate the porous poly(lactic-acid)-*co*-(trimethylene-carbonate)/poly(glycolic-acid)-*co*-(trimethylene-carbonate) scaffolds with uniform microstructure by the 3D extrusion printing technology in a mild printing condition. The physicochemical properties of the poly(lactic-acid)-*co*-(trimethylene-carbonate)/poly(glycolic-acid)-*co*-(trimethylene-carbonate) and the 3D printing scaffolds were investigated by universal tensile dynamometer, fourier transform infrared reflection (FTIR), scanning electron microscope (SEM) and differential scanning calorimeter (DSC). Meanwhile, the degradability of the PLLA-TMC/GA-TMC was performed *in vitro* degradation assays. Compared with PLLA-TMC group, PLLA-TMC/GA-TMC groups maintained the decreasing T_g, higher degradation rate and initial mechanical performance. Furthermore, the PLLA-TMC/GA-TMC 3D printing scaffolds provided shape-memory ability at 37 °C. In summary, the PLLA-TMC/GA-TMC can be regarded as an alternative substitution material for bone tissue engineering.

Bone defects beyond the self-healing size caused by trauma infection, osteomatosis and osteoporosis are major public safety problems that need to be solved urgently in clinical practice [1–4]. Under the guidance of physicochemical properties of the bone and bone healing process, an ideal biodegradable substitution material should possess the similar mechanical properties with bone tissue and a degradation rate that matches the growth of bone tissue [5,6]. Moreover, it should provide the similar structure and function with natural bone but with non-immunogenicity and nontoxic [6,7]. Hence, the main challenge for designing an ideal biodegradable bone substitution material is to precise control of the degradation time, degradation behavior, mechanical properties and processability of the implantation materials.

Among these biodegradable substitution materials, biodegradable polymers, such as polylactic acid, poly(glycolic acid), poly(caprolactone), poly(trimethylene carbonate) and poly(hydroxyalkanoate) (referred to as PLA, PGA, PCL, PTMC and PHA hereafter) have attracted a lot of focus due to their excellent processing properties, manageability, controllable degradation rate and good biocompatibility [8–10].

Nevertheless, a single synthetic degradable polymer material used as bone repair scaffold is unable to meet all the application

* Corresponding authors.
E-mail addresses: xiongcdcioc@163.com (C. Xiong), Likainan1961@126.com (K. Li).

https://doi.org/10.1016/j.cclet.2022.04.049
1001-8417/

requirements as a faultless bone repairing biomaterial [11]. For instance, though PLLA was commonplace in the field of implantable devices [12,13], it is remained an on-going challenge to accelerate its degradation rate and reduce its acidic degradation products, which is extremely important for applications in bone regeneration [14,15].

In our previous work, we have applied poly(lactic acid-*co*-trimethylene carbonate) (PLLA-TMC) to the preparation of bone repair materials and scaffolds. We found that with the increase of trimethylene carbonate (referred to as TMC hereafter) content, the acid degradation products of the materials decreased and the surface corrosion degradation behavior became more obvious. At the same time, PLLA-TMC has long been used in the study of artificial blood vessels because of its excellent shape memory function under body temperature [16,17]. Although PLLA-TMC has good shape memory function and unique surface corrosion degradation behavior, which is contributed to better carry out minimally invasive orthopedic implantation and maintain the dimensional stability of orthopedic implant instruments, the problems of long degradation time and low elastic modulus still need to be further solved [18–20]. Poly(glycolic acid-*co*-trimethylene carbonate), a biodegradable material with rapid degradation rate and distinguished mechanical properties, which is widely used in absorbable surgical suture [21] and tissue engineering [22] may be an ideal strategy to deal with this problem.

Aiming to achieve the therapy of bone defect, we designed an innovative biodegradable composite by blending the PGA-TMC into PLLA-TMC to accelerate the degradation rate and improve the mechanical properties. In this study, the PLLA-TMC/GA-TMC with different blending ratios were systematically investigated the physicochemical properties, *in vitro* degradation behavior, biocompatibility and shape memory ability. To functionalize the PLLA-TMC/GA-TMC porous scaffold with the personalized customization of the external shape, internal macro-porous structure and surface microporous structure of the scaffold, we fabricate the scaffold *via* 3D extrusion printing technology in a mild condition. The mechanical properties, surface and internal morphology and pore size of the scaffolds were thoroughly explored according to relative assays. To the best of our knowledge, this is the first example to prepare the porous scaffold based on PLLA-TMC *via* low temperature 3D extrusion method for bone regeneration.

Methods and the composite material group list (Fig. S1) can be found in Supporting information. Figs. 1a and b showed the surface and cross section morphology of CP1, CP2, CP3 and CP4 splines. The results showed all the groups possessed the surface with winkles which was similar with PTMC. With the addition of GA-TMC content, the cross section of splines became smoother. In addition, phase interface of CP2-CP4 were not obvious, which resulted in the blending components contain the same proportion of TMC and have good compatibility. FTIR spectra of CP1, CP2, CP3 and CP4 were shown in Fig. 1c. In the spectrum of all groups, it revealed characteristic absorption bands of its LLA-TMC structure, 2908 cm^{-1} (C—H stretching), 1751 cm^{-1} (C=O stretching), 1267 cm^{-1} (C—O stretching) and 1191 cm^{-1} (C—O—C stretching). In addition, the characteristic peak of GA-TMC could be observed at 1455 cm^{-1}, which assigned to be the CH_2 in GA-TMC. All of the groups were detected only a T_g, which demonstrated that PLLA-TMC and PGA-TMC were amorphous polymers. Moreover, the T_g of CP1 was 29.43 °C. However, the T_g of the other groups decreased slightly due to the incorporation of GA-TMC (Fig. 1d).

Generally speaking, under the condition of maintaining blood supply and stable fixation, the bone healing time is about 3 months. In this study, PBS hydrolysis degradation was performed (up to 10 weeks) to investigate the *in vitro* degradation behavior of the PLLA-TMC/GA-TMC. The mass loss assay showed that the blend of GA-TMC significantly enhanced the degradation rate

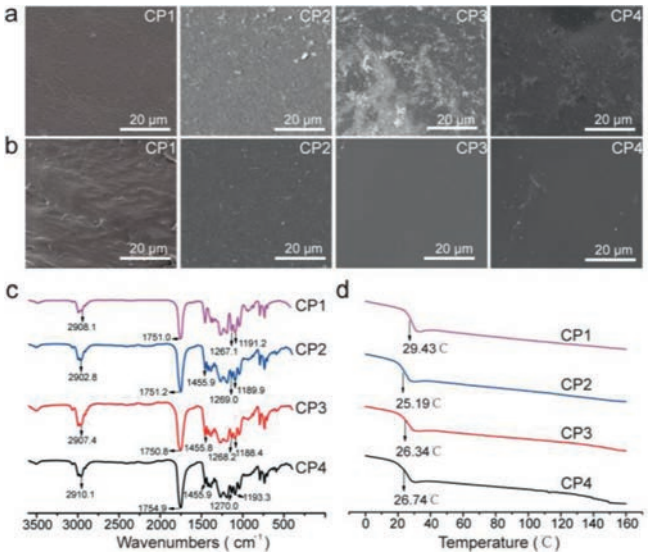

Fig. 1. The physicochemical propeties of PLLA-TMC and PLLA-TMC/GA-TMC. (a) The surface morphology of CP1-CP4. (b) The surface and cross section morphology of CP1-CP4. (c) The FTIR spectra of CP1-CP4. (d) The DSC results of CP1-CP4.

(Fig. 2a). The mass loss ratio of CP1 was only 5.36%, while 31.82% for CP2 (at 10 weeks). After 10 weeks degradation, CP3 and CP4 splines showed the imilar degradation behavior with pure PTMC and exhibited a tendency to creep [23,24], while there was no curling before, and the dimensional stability was maintained. However, dimensional stability plays an important role in the process of bone repair, because the scaffold needs to bear a certain supporting role in the early stage of healing, especially before callus shaping stage (8–12 weeks) [25]. This result also confirmed the rationality of our blend materials in the preparation of bone repair scaffolds. The water absorption of CP1 was the minimum (7.64% for 6 weeks), whereas 22.34% for CP2, 25.09% for CP3, 28.39% for CP4. The results of water absorption and mass loss assured that the GA-TMC promoted the degradation. With increasing content of GA-TMC, the initial tensile strength and break elongation of the composite groups increased significantly. Meanwhile, the results of SEM showed that the internal degradation of the spline increased with the increase of GA-TMC content, which was different from the surface corrosion degradation of pure PLLA-TMC (Fig. 2b). In previous study, we found PLLA-TMC7030 is mainly degraded by surface dissolution within eight weeks of PBS degradation experiment, and showed a degradation behavior accompanied by internal collapse and surface dissolution eight weeks later [19]. Therefore, this phenomenon also confirmed that the introduction of GA-TMC accelerated the degradation rate of the blending material.

Fig. 3a displayed the surface and section microphotograph of 3D scaffolds of CP4 detected by optical stereomicroscope. It clearly showed that CP4 scaffold possess 3D multilayered tubular architecture along with the uniform alignment and pore size. Average pore size of CP4 scaffold with internal connected macroporous structure was calculated about 403.12 ± 10.68 μm (from 200 μm to 500 μm), that were beneficial to differentiation and growth of bone cell lines and soft tissues, and provided ostoconduction (Table 1) [26,27]. In particular, the preparation of printing ink and its properties including flow and molding will significantly affect the application of biological extrusion 3D printing, a fast and efficient preparation technology. Therefore, we utilized DCM solvent to prepare printing ink, and use its rapid volatilization to assist scaffold forming. Meanwhile, due to the fast volatilization rate of DCM in the printing process, a large number of micropores with a pore size of about 5 μm were produced on the surface of the scaf-

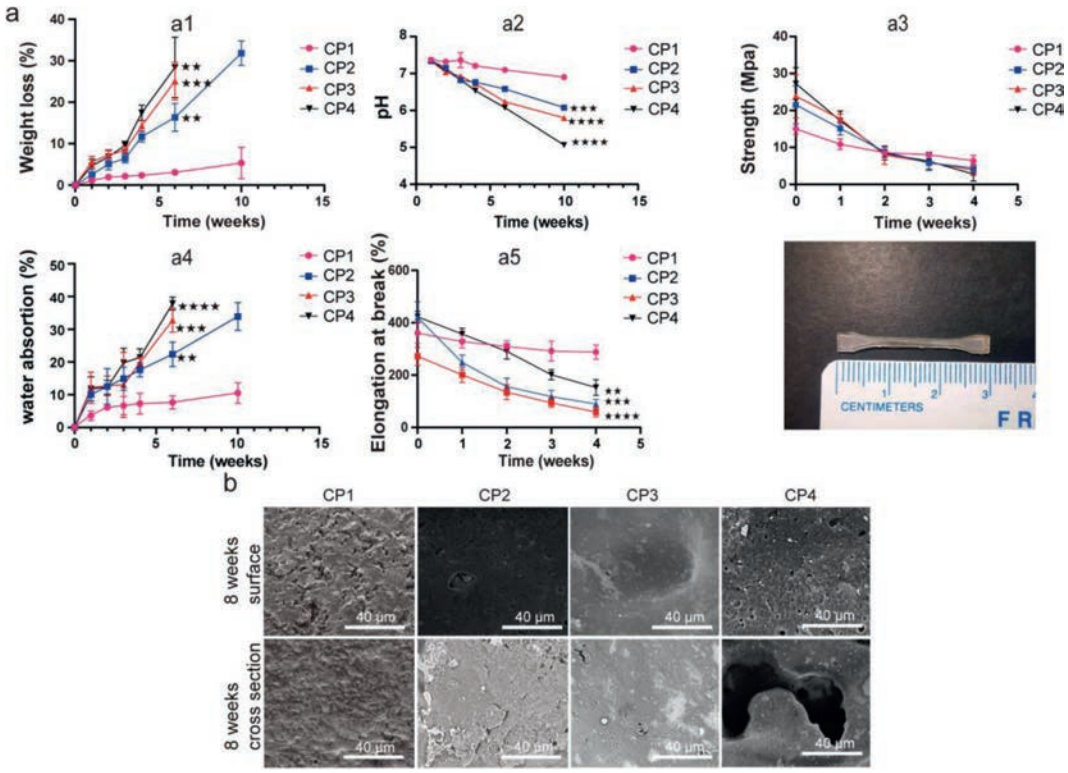

Fig. 2. The hydrolytic degradation of PLLA-TMC and PLLA-TMC/GA-TMC (a): weight loss (a1); pH value (a2); tensile strength (a3); water absorption (a4); break elongation (a5). (b) Cross section morphology.

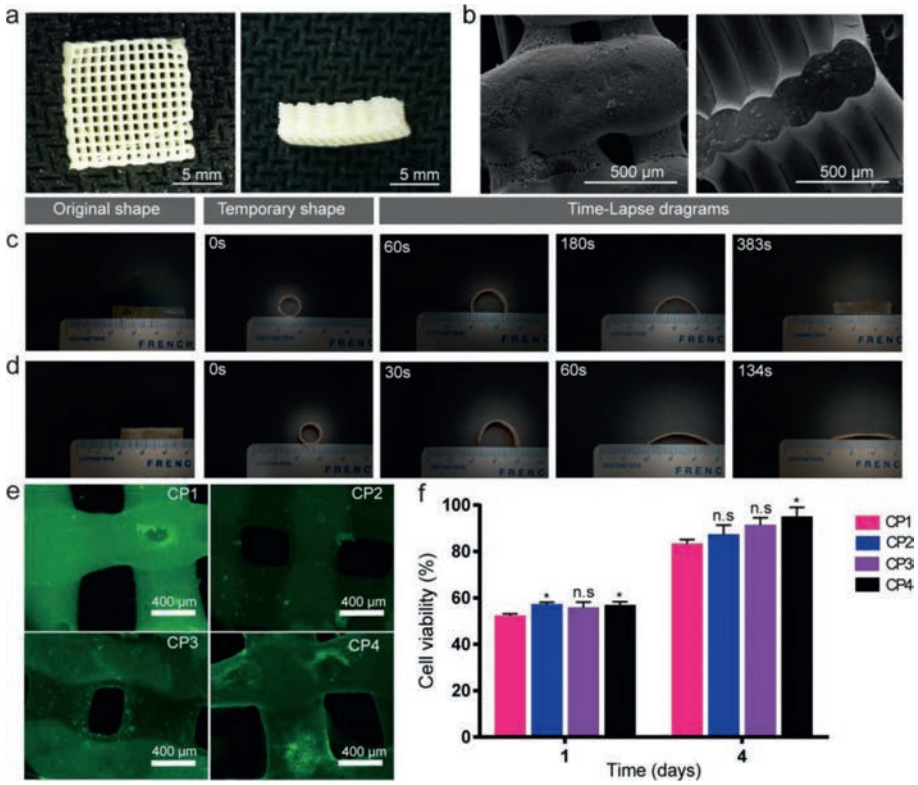

Fig. 3. Optical microscope (a) and SEM (b) pictures of CP1 scaffolds; shape memory ability of CP1 (c) and CP4 (d) splines; (e) osteoblast fluorescence detection (7 days); (f) cytotoxicity of scaffolds (1 day and 4 days).

Table 1
Physical property of indicated scaffolds.

	Total porosity for scaffolds (%)	Compressive modulus (MPa)	Average micro pore size (μm)	Average macro pore size (μm)
CP1	58.00 ± 1.15	78.00 ± 10.36	5.73 ± 1.25	371.31 ± 12.71
CP2	53.45 ± 2.05	84.03 ± 6.97	6.01 ± 0.92	392.55 ± 17.31
CP3	61.24 ± 2.02	105.27 ± 7.35	3.99 ± 2.91	387.92 ± 8.99
CP4	56.00 ± 2.02	106.71 ± 8.34	4.23 ± 2.16	403.12 ± 10.68

fold (Table 1). To add more, the rough surface of CP4 3D printed scaffolds with micro-holes structure were expressly discovered in Fig. 3b which was resulted in the solvent volatilization during extrusion printing. It is evident that high surface area and rough surface of the implant scaffold availed the proliferation and adhesion of cells [28–30]. Compared to microsphere scaffold (<40%) [31], total porosity for CP4 scaffold could obviously increase to 56% ± 2.02%. However, the actual porosity was obviously lower than the theoretical value (70%) due to the extruded material will collapse slightly due to gravity during solvent volatilization, solidification and molding, resulting in over dense accumulation.

With the development of clinical technology and material science, doctors and scientists are constantly pursuing minimally invasive surgery and personalized customization of implants in order to obtain better curative effect and reduce surgical trauma. Shape memory polymers (SMPs) are driving interests in minimally invasive surgery and bone tissue engineering filed, especially under challenging spatial implantation. SMPs would deform into a temporary shape in implantation progress, and revert back original shape received the stimulus (for example temperature) [32]. In this work, we tested the shape memory effect of CP1 and CP4 under 37 °C (similar to human body temperature). It is distinctly showed that the temporary cylindrical shape of CP4 recovered rectangle permanent shape within 134 s (Fig. 3d), while CP1 needed a relatively longer time to recover (323 s) (Fig. 3c). Namely, the shape recover time that allows surgeons to complete implant, could be controlled by PLLA-TMC and PGA-TMC component ratio. Another key indicator for biodegradable scaffolds is biocompatibility. MC3T3-E1 cells adhered and proliferated well on CP1, CP2 and CP4 3D printed scaffolds and the number of cells increased gradually during culture period (Fig. 3e). On the one hand, this result showed that the scaffold material has good biocompatibility; on the other hand, the microporous structure on the surface of the scaffold was also conducive to cell adhesion and proliferation. Cell viability results revealed CP1, CP2 and CP4 scaffolds possess good biocompatibility (Fig. 3f).

In summary, we designed a novel bone substitution material by blending PLLA-TMC with PGA-TMC. The results showed the tensile strength was significantly increased with the addition of GA-TMC. On the contrary, the T_g and break elongation of the splines were slightly decreased with the increasing content of GA-TMC. More importantly, compared to the PLLA-TMC, the addition of GA-TMC distinctly promoted the hydrolytic degradation rate and shape recover time. We adopted a low temperature way to fabricate the porous scaffolds (CP1 and CP4) *via* 3D printing machine with uniform internal connected porous structure, rough surface, suitable mechanical properties and high porosity. To sum up, the novel shape memory 3D printed PLLA-TMC/GA-TMC scaffold with improved biodegradability, mechanical properties is promising to be used in clinic to repair the bone defect in the future. However, due to the influence of gravity in the forming process, the porosity of this low-temperature printing method will be lower than the ideal value. In the subsequent research, we can further reduce the ice plate temperature in the printing process to freeze the solvent or print at room temperature to speed up the solvent volatilization speed, so that the actual porosity and structure are closer to the ideal state. Meanwhile, in the follow-up work, we can further examine the degradation and osteogenesis of the system scaffold in animal models.

Declaration of competing interest

The authors declare that they have no known competing financial interests or personal relationships that could have appeared to influence the work reported in this paper.

Acknowledgments

The authors are grateful for the sub project of the national major project generation method and application verification of personalized rehabilitation prescription for patients with balance (No. 2019YFB1311403).

Supplementary materials

Supplementary material associated with this article can be found, in the online version, at doi:10.1016/j.cclet.2022.04.049.

References

[1] C. Chen, Y. Li, X. Yu, et al., Chin. Chem. Lett. 29 (2018) 1609–1612.
[2] D.W.J.B. Hutmacher, Biomaterials 21 (2000) 2529–2543.
[3] S.K.L. Levengood, M.J.J.o.M.C.B. Zhang, J. Mater. Chem. B 2 (2014) 3161–3184.
[4] J.R. Mauney, C. Jaquiéry, V. Volloch, et al., Biomaterials 26 (2005) 3173–3185.
[5] K. Rezwan, Q.Z. Chen, J.J. Blaker, A.R. Boccaccini, Biomaterials 27 (2006) 3413–3431.
[6] A.J. Salgado, O.P. Coutinho, R.L. Reis, Macromol. Biosci. 4 (2004) 743–765.
[7] T. Jiang, W.I. Abdel-Fattah, C.T. Laurencin, Biomaterials 27 (2006) 4894–4903.
[8] W. Amass, A. Amass, B.J.P.I. Tighe, Polym. Int. 47 (1998) 89–144.
[9] D.K. Gilding, A.M. Reed, Polymer 20 (1979) 1459–1464.
[10] L.S. Nair, C.T. Laurencin, Prog. Polym. Sci. 32 (2007) 762–798.
[11] Q. Wang, J. Xu, H. Jin, et al., Chin. Chem. Lett. 28 (2017) 1801–1807.
[12] J.E. Bergsma, J. Oral. Maxil. Surg. 56 (1998) 614–615.
[13] B. Buntner, M. Nowak, J. Kasperczyk, et al., J. Control. Release 56 (1998) 159–167.
[14] S. Lee, H. Shin, Adv. Drug Deliv. Rev. 59 (2007) 339–359.
[15] M.F. Maitz, Biosurf. Biotribol. 1 (2015) 161–176.
[16] J. Hua, K. Gebarowska, P. Dobrzynski, et al., J. Polym. Sci. Pol. Chem. 47 (2009) 3869–3879.
[17] A.C. Motta, V. de Miranda Fedrizzi, M.L.P. Barbo, E.A.R. Duek, Polym. Bull. 75 (2018) 4515–4529.
[18] X. Hu, J. He, X. Yong, et al., Colloids Surf. B: Biointerfaces 195 (2020) 111218.
[19] X. Hu, S. Mi, J. Lu, et al., Colloids Surf. A: Physicochem. Eng. Asp. 615 (2021) 126220.
[20] S. Mi, X. Hu, Z. Lin, et al., Colloids Surf. A: Physicochem. Eng. Asp. 622 (2021) 126594.
[21] C. Sanson, C. Schatz, J.Le Meins, et al., Langmuir 26 (2010) 2751–2760.
[22] A.H.K. Chou, R.Z. LeGeros, Z. Chen, Y. Li, Implant Dent. 16 (2007) 89–100.
[23] O. Guillaume, M.A. Geven, C.M. Sprecher, et al., Acta Biomater. 54 (2017) 386–398.
[24] A.P. Pêgo, D.W. Grijpma, J. Feijen, Polymer 44 (2003) 6495–6504.
[25] P.V. Giannoudis, T.A. Einhorn, D. Marsh, Injury 38 (2007) S3–S6.
[26] O. Gauthier, J. Bouler, E. Aguado, et al., Biomaterials 19 (1998) 133–139.
[27] K. Huang, G. Liu, Z. Gu, J. Wu, Chin. Chem. Lett. 31 (2020) 3190–3194.
[28] J. Amirian, N.T.B. Linh, Y.K. Min, B. Lee, Int. J. Biol. Macromol. 76 (2015) 10–24.
[29] J. Davies, Anat. Rec. 245 (1996) 426–445.
[30] C.A. Vacanti, J.P. Vacanti, R. Langer, ACS Symp. Ser. 540 (1993) 16–34.
[31] C. Sanson, C. Schatz, J.F. Le Meins, et al., J. Control. Release 147 (2010) 428–435.
[32] Q. Zhao, J. Wang, H. Cui, et al., Adv. Funct. Mater. 28 (2018) 1801027.